**Title**

Fatquant: An automated image analysis tool for identification of fat cells in heterogeneous hematoxylin and eosin tissue sections.

**Authors**

Roshan Ratnakar Naik[1], Annie Rajan[2], Nehal Kalita[3]

**Affiliations**

[1] Dr. Roshan Ratnakar Naik, Guest Faculty, Dnyanprassarak Mandal's College and Research Centre, Assagao, Khorlim, Mapusa-Goa, 403507. ORCID ID: 0000-0003-4515-871X. Email address: ros007swa@gmail.com

[2] Mrs. Annie Rajan, Associate Professor, Department of Computer Science and Technology, Dhempe College of Arts and Science, Miramar, Panaji-Goa, 403 001. ORCID ID: 0000-0001-6201-2654. Email address: ann_raj_2000@yahoo.com

[3] Nehal Kalita, M.Sc. Computer Science. ORCID ID: 0000-0001-6997-5621. Email address: nehalkalita94@gmail.com

Corresponding Author: Dr. Roshan R. Naik

## Author contributions

R.R.N. conceptualized the idea and wrote the manuscript.

A.R. conceptualized the idea.

N.K. formulated the mathematical approach and wrote the Python programs.


## Abstract

Hematoxylin and eosin (H and E) is one of the common histological staining techniques that provides information on the tissue cytoarchitecture. Adipose (fat) cells accumulation in pancreas has been shown to impact beta cell survival and its endocrine function. The current automated tools available for fat analysis are suited for white adipose tissue which is homogeneous and easier to segment unlike heterogeneous tissues such as pancreas where fat cells continue to play critical physiopathological functions. In the current study, we present an automated fat analysis tool, Fatquant, where mathematical formula to calculate diagonal of a square drawn inside circle is utilized for identification and analysis of fat cells in heterogeneous H and E tissue sections. Using histological images of pancreas from a publicly available database, we show an area accuracy overlap of 89-93% between manual versus automated algorithm based fat cell detection.



## Keywords

Adipose or fat cells, Hematoxylin and Eosin, image processing, tissue segmentation.

**Author Summary**

We have developed an automated tool, Fatquant, for identification of fat cells in complex hematoxylin and eosin tissue sections such as pancreas which can aid the pathologist for detection and analysis. Fatquant is unique as current fat automated tools work well for homogeneous white adipose tissue but not for other tissue samples.

## Introduction

Hematoxylin and eosin (H & E) is a widely used histological tissue staining technique for medical diagnosis and scientific research. Hematoxylin stains cell nuclei blue while eosin stains the cytoplasm and connective tissue pink thus allowing microscopic differentiation of tissue cytoarchitecture in sections. The analysis involves manual examination by pathologist to ascertain presence/absence of disease markers and or grading of disease progression which is semi-quantitative and subjective in nature [1]. Obesity is characterized by increased adipocyte or fat cell numbers and enlargement (change in diameter) due to lipid accumulation leading to increase in white adipose cellular mass [2, 3]. However, in recent years, the role of fat cells in pathophysiology of liver, pancreatic and lung disease is increasingly recognized due to close interaction with their corresponding endocrine cells [4-6]. To complement the current manual assessment, several digital tools have been developed such as CellProfiler [7], Adiposoft [8], and Adipocount [9]. However, they cannot efficiently identify fat cells in complex tissues such as liver, pancreas, lung as white adipose tissue is generally homogeneous making tissue segmentation relatively easier [10]. Usually, these algorithms involve splitting the image into various colour channels with the red channel binarized using automatic thresholding method to separate the bright pink fat areas from dark purple-bluish cell nuclei. Subsequently, a watershed

algorithm is applied to fillup missing fat cell membrane and improve cell count [8, 9]. The output of these processes include the labels and statistical analysis of individual cells. These tools have been successfully applied to white adipose tissue, however, other organs like liver, pancreas, lungs have been challenging due to hetergeneous cell types. Previously, we have used tile rendering approach for profile analysis from three dimensional spatial data [11] as it reduces time complexity by considering only a portion of an image at a time. In the current study, we have developed an automated tool, Fatquant, in which the fat cells were identified in processed images by calculating the diagonal of a square circumscribed by circle.

## Results

The Table 1 provides fat cell area accuracy in percentage with yellow and blue denoting manual and algorithm based detection, respectively. While the green represents overlapping fat cell area accuracy.

**Table 1: Percent area accuracy of overlapping fat cells**

| Figure | Threshold value | Min. diameter | Max. diameter | Area accuracy (%) |
|---|---|---|---|---|
| 8 (c) | 234 | 27 | 115 | 89.70 |
| 9 (c) | 228 | 25 | Null | 93.04 |
| 10 (c) | 228 | 29 | Null | 90.64 |

From Table 1, it can be noted that Figure 8 (c) and Figure 10 (c) show less accuracy as compared to Figure 9 (c) because fat cells in these two images have more overlaps with other artifacts or fat cells excluded when it touches the boundary.

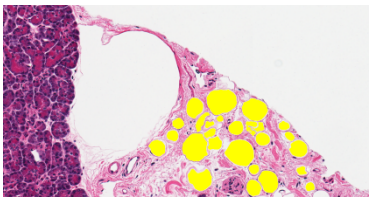

**Figure 8 (a)**

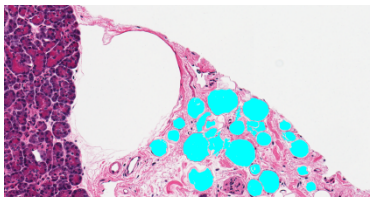

**Figure 8 (b)**

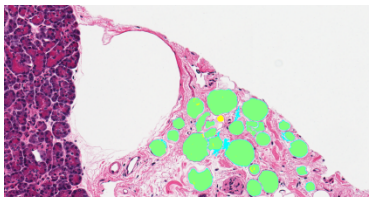

**Figure 8 (c)**

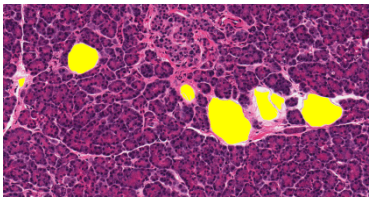

**Figure 9 (a)**

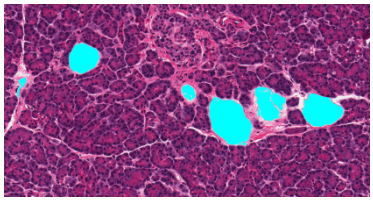

**Figure 9 (b)**

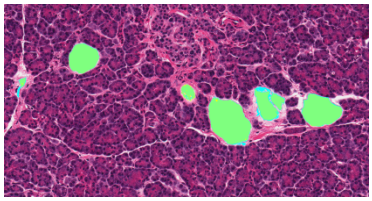

**Figure 9 (c)**

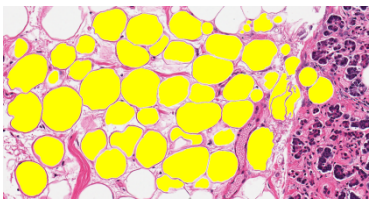

**Figure 10 (a)**

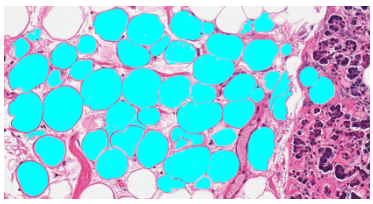

**Figure 10 (b)**

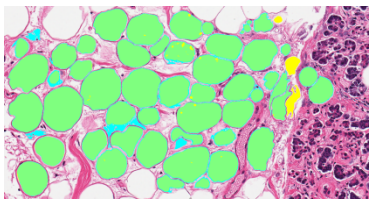

**Figure 10 (c)**

Figure 8-10: Comparison of a) manual (yellow) vs. b) algorithm (blue) based image analysis and c) green represents overlapping fat cells identified through the two approaches.

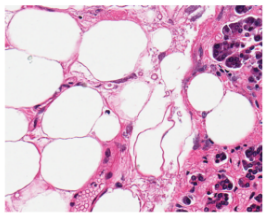

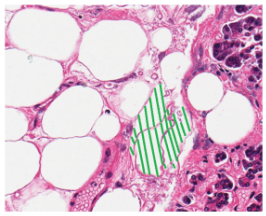

**Figure 11 (a)**

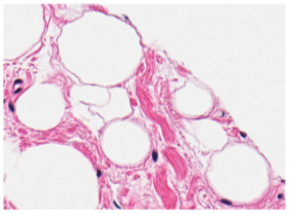

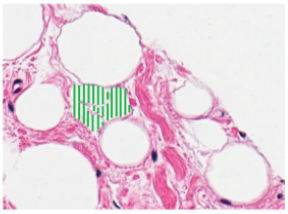

**Figure 11 (b)**

Figure 11 (a) and (b) below depicts deformed fat cell membrane likely due to tissue processing steps with green shaded areas representing neighbouring cells that give impression of single spherical or oval fat cells.

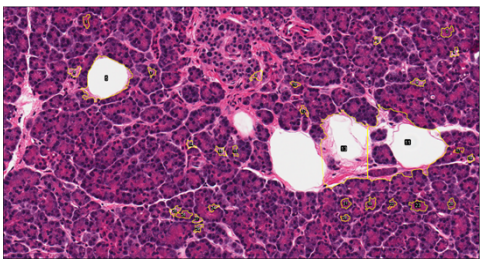

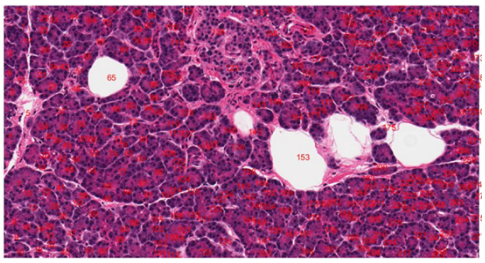

**Figure 12 (a)** **Figure 12(b)**

Figure 12 (a) and Figure 12 (b) are Adiposoft and Adipocount outputs, respectively obtained with pancreas H and E stained image. Note, the corresponding output obtained for same image with Fatquant tool in Figure 9 (b). AdipoCount does not require any input parameter. Parameters for Adiposoft used were minimum diameter (25) and maximum diameter (3000).

## Discussion

We have developed a tool, Fatquant, to identify fat cells in heterogeneous histological tissue sections that can complement work of pathologist in identification and analysis of fat cells due to their growing importance in pathophysiological functions and with the availability of whole slide digitized images it can save significant amount of time. We observed an overlapping area accuracy ranging between 89- 93% in manual versus automated Fatquant based detection indicating good concordance with variation due to possible artifacts during tissue processing, or peripheral cells excluded due to incomplete cells. The 10% loss in accuracy is mostly because of two reasons. One reason is valid fat cells getting overlapped with other white coloured tissue material or the background which adds extra area to detected fat cells. Another reason is some fat cells having nucleus or other dark coloured tissue inside them which restricts fat cells getting detected as per minimum diameter.

## Materials and Methods

The H and E images for the analysis were downloaded from a publicly accessible Genotype-Tissue Expression (GTEx) Portal (Broad Institute, Cambridge, MA, USA) using the Histology Viewer tool [12]. The GTEx tissue image library contains high-resolution histology images for various tissue types from several postmortem donors. Spherical or oval white spaces were categorized as fat (adipose) cells while large and irregular white spaces were grouped as artifacts. A sample size of three high resolution pancreas histology images were analyzed with sample IDs GTEX-11DXZ-0826, GTEX-1122O-0726, GTEX-1117F-1726. The images have magnification of 20x (0.4942 mpp—microns per pixel) [13]. The source code was written in Python version 3.8.0 (Python Software Foundation, Beaverton, Oregon, USA) with Core i7 3rd Generation CPU, 8 GB RAM and Intel HD graphics 4000 GPU.

## Image processing

The following steps were utilized for image analysis:

1. Binary thresholding of input image.
2. Segmentation of white pixels from thresholded image.
3. Selection of segments for fats as per range of diameter.
4. Removal of fats from boundary.
5. Analysis.

These steps are described as follows:

1. Binary thresholding of input image

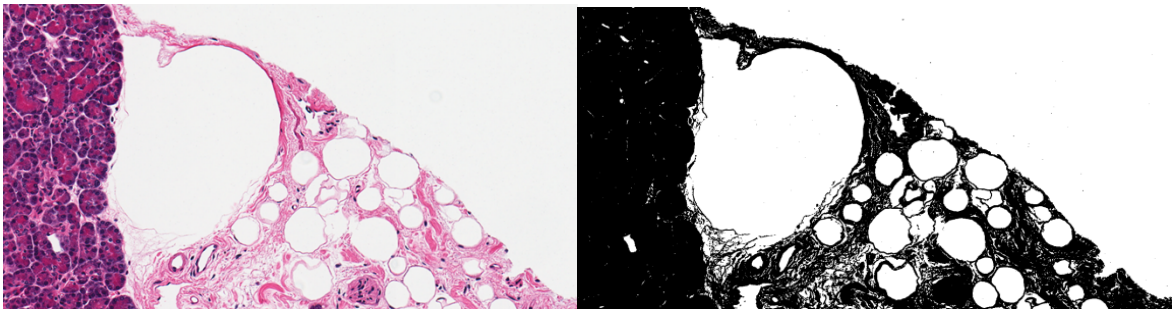

**Figure 1: a) Input image, b) binary thresholded image.**

Binary thresholding is performed on input image (**Figure 1a)** by referring the grayscale values of each pixel. The system relies on a parameter value which ranges from 0 to 255 to identify the limit of each color. Pixels with grayscale values below the parameter are considered as black and above the parameter as white with the binary thresholded image (**Figure 1b**) having parameter value set as 230.

2. Segmentation of white pixels from thresholded image

White pixels are initially segmented by combining tile rendering with scanline rendering and then identifying possible merge of segments in a tile with their immediate neighbours. The input image is divided into multiple square tiles each with length 100 pixels and then scanline rendering is performed within each tile to identify white pixels and form possible segments with their neighbours on left or top (**Figure 2a, 2b**). Once scanline rendering is performed till the last row of a tile then the identified segments are merged on the basis of their horizontal and vertical neighbors (**Figure 2c**).

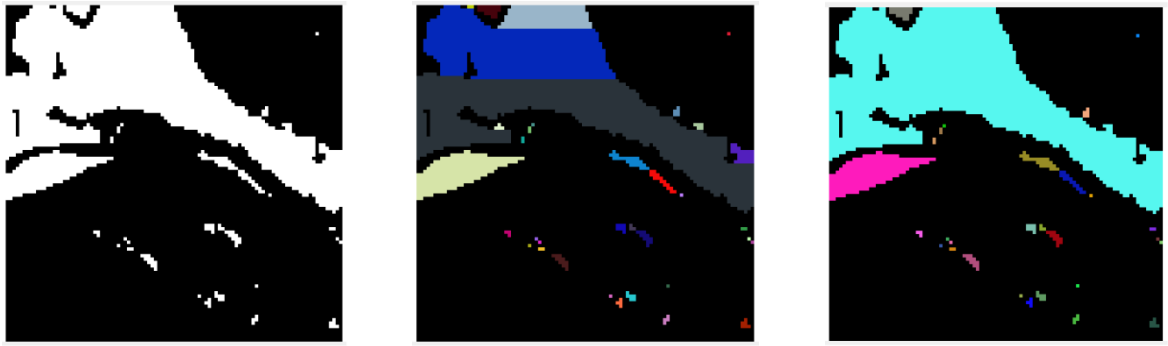

**Figure 2 (a)** **Figure 2 (b)** **Figure 2 (c)**

**Figure 2:** Segmentation of white pixels in thresholded image with possible segments with neighbours on (a) left, (b) top, (c) identified segments merged.

Segments which have only diagonal neighbours with another segment and not horizontal or vertical, are not merged. **Figure 3** and **4** shows segments within tiles and fully merged segments of the thresholded image respectively. Varying colours in the images represent different segments.

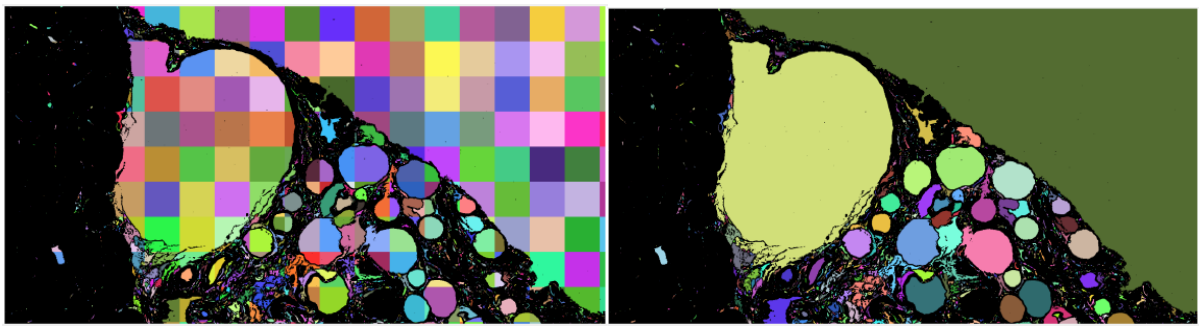

**Figure 3**: Segments within tiles. **Figure 4:** fully merged segments of thresholded images with variegated colours as different segments.

3. Selection of segments for fats as per range of diameter

White segments are considered as probable fats if a square kernel of diagonal length equal to length of assigned diameter value fits anywhere within their boundary. This square can be

assumed as the largest square that can get inscribed in a circle of input diameter values. Side length of a square, can be calculated as:

$s = \frac{d}{\sqrt{2}}$, where s = square side length; d = diameter. The system makes use of minimum and maximum diameter values to select fats. The system first refers minimum value to select segments whose area need not be narrow everywhere (**Figure 5a)** and then refers maximum value to discard the segments of the selected list having a very wide area (**Figure 5b**).

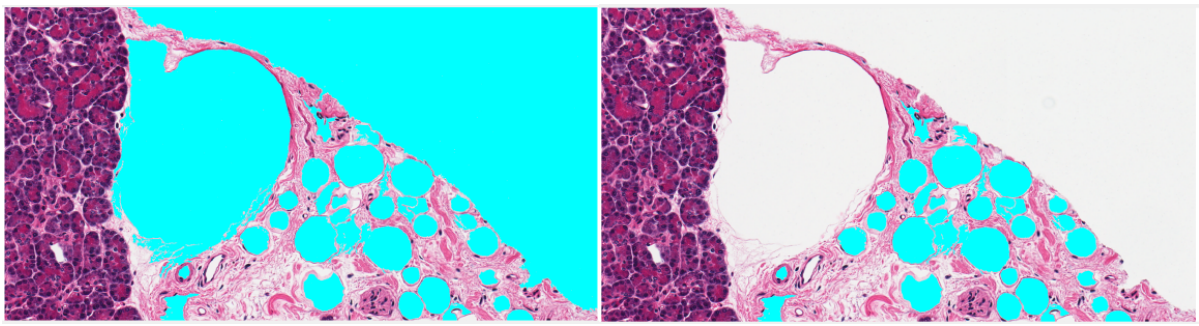

Figure 5: Selection of fat using a) minimum and b) maximum diameter values.

Before traversing by a square kernel to find probable valid segments, the system determines the smallest dimension that encompasses all of the image's segments (**Figure 6a, 6b**). Because the kernel's position is only updated by one pixel (horizontally or vertically) every iteration, determining the smallest dimension for traversal reduces the time complexity.

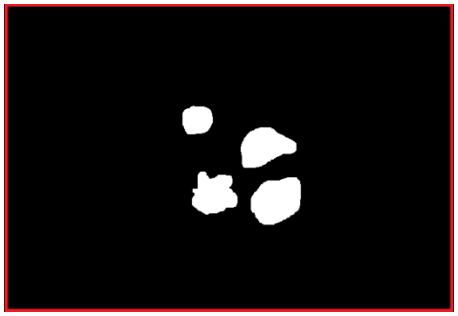

**Figure 6a**

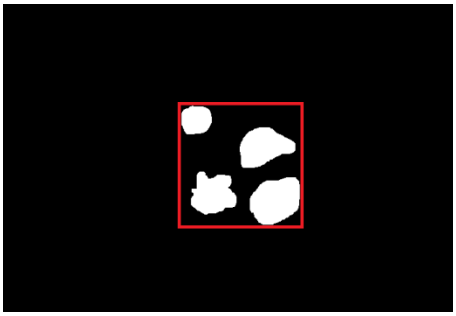

**Figure 6 b**

Figure 6: a) and b) Determination of smallest dimension that covers all image segments.

4. Removal of fats from boundary

Segments which are identified as fats but touch pixels in boundary are discarded because their entire size is not known within the dimension of input image (**Figure 7**). Some of these segments may even get discarded while selecting segments as per diameter.

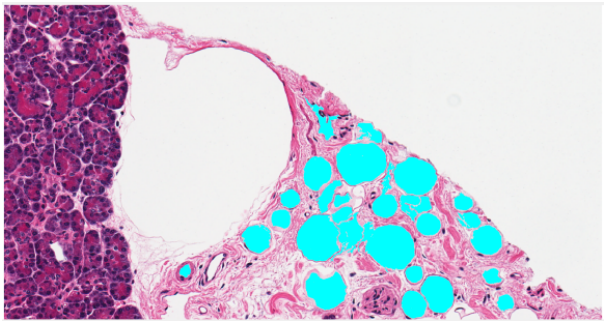

**Figure 7:** Fat cell removed from peripheral boundary.

5. Analysis

The machine annotated fat segments were compared with human annotated fat segments to check the validity of our image analysis algorithm. If machine and human annotated segments have pixels in common then, those pixels are considered as valid. The accuracy of the output in terms of area covered is calculated as:

$$AC = \frac{Av}{(Av + (Ah - Av) + (Am - Av))}$$

, where AC = valid area accuracy; Av = total valid area; Ah = total human annotated area; Am = total machine annotated area.

**Acknowledgments**

There is no potential conflicts of interest and no funding to declare. The datasets generated are not publicly available as they are part of ongoing work to identify more cell types in complex H and E histology sections. The source code can be made available based upon reasonable request to the authors.

## References


[1] Gurcan, M. N., Boucheron, L. E., Can, A., Madabhushi, A., Rajpoot, N. M., & Yener, B. (2009). Histopathological image analysis: a review. *IEEE Rev Biomed Eng, 2*, 147-171. doi: 10.1109/RBME.2009.2034865.

[2] Jo, J., Gavrilova, O., Pack, S., Jou, W., Mullen, S., Sumner, A. E., . . . Periwal, V. (2009). Hypertrophy and/or Hyperplasia: Dynamics of Adipose Tissue Growth. *PLoS Comput Biol, 5*(3), e1000324. doi: 10.1371/journal.pcbi.1000324.

[3] Longo, M., Zatterale, F., Naderi, J., Parrillo, L., Formisano, P., Raciti, G. A., . . . Miele, C. (2019). Adipose Tissue Dysfunction as Determinant of Obesity-Associated Metabolic Complications. *Int J Mol Sci, 20*(9). doi: 10.3390/ijms20092358.

[4] Ntikoudi, E., Kiagia, M., Boura, P., & Syrigos, K. N. (2014). Hormones of adipose tissue and their biologic role in lung cancer. *Cancer Treat Rev, 40*(1), 22-30. doi: 10.1016/j.ctrv.2013.06.005

[5] Pacifico, L., Di Martino, M., Anania, C., Andreoli, G. M., Bezzi, M., Catalano, C., & Chiesa, C. (2015). Pancreatic fat and beta-cell function in overweight/obese children with nonalcoholic fatty liver disease. *World J Gastroenterol, 21*(15), 4688-4695. doi: 10.3748/wjg.v21.i15.4688

[6] Gerst, F., Wagner, R., Oquendo, M. B., Siegel-Axel, D., Fritsche, A., Heni, M., . . . Ullrich, S. (2019). What role do fat cells play in pancreatic tissue? *Mol Metab, 25*, 1-10. doi: 10.1016/j.molmet.2019.05.001.

[7] Carpenter, A. E., Jones, T. R., Lamprecht, M. R., Clarke, C., Kang, I. H., Friman, O., . . . Sabatini, D. M. (2006). CellProfiler: image analysis software for identifying and quantifying cell phenotypes. *Genome Biol, 7*(10), R100. doi: 10.1186/gb-2006-7-10-r100.

[8] Galarraga, M., Campion, J., Munoz-Barrutia, A., Boque, N., Moreno, H., Martinez, J. A., . . . Ortiz-de-Solorzano, C. (2012). Adiposoft: automated software for the analysis of white adipose tissue cellularity in histological sections. *J Lipid Res, 53*(12), 2791-2796. doi: 10.1194/jlr.D023788.

[9] Zhi, X., Wang, J., Lu, P., Jia, J., Shen, H. B., & Ning, G. (2018). AdipoCount: A New Software for Automatic Adipocyte Counting. *Front Physiol, 9*, 85. doi: 10.3389/fphys.2018.00085.

[10] Glastonbury, C. A., Pulit, S. L., Honecker, J., Censin, J. C., Laber, S., Yaghootkar, H., . . . Lindgren, C. M. (2020). Machine Learning based histology phenotyping to investigate the epidemiologic and genetic basis of adipocyte morphology and cardiometabolic traits. *PLoS Comput Biol, 16*(8), e1008044. doi: 10.1371/journal.pcbi.1008044.

[11] Maurya, R.K., Kulkarni, S.T., & Kalita, N. (2018). Projection-Based Spatial Morphology for Extracting Ridge and Valley Profiles of Mountains from 3D Amorphous Data. *2018 4th International Conference on Computing Communication and Automation (ICCCA)*, 1-6.

[12] Consortium, G. TEx. (2015). Human genomics. The Genotype-Tissue Expression (GTEx) pilot analysis: multitissue gene regulation in humans. *Science, 348*(6235), 648-660. doi: 10.1126/science.1262110.

[13] Badea, L., & Stanescu, E. (2020). Identifying transcriptomic correlates of histology using deep learning. *PLoS One, 15*(11), e0242858. doi: 10.1371/journal.pone.0242858.